Robust Signal Processing for GNSS

Daniele Borio

European Commission, Joint Research Centre (JRC), Ispra (VA), Italy
Email: {daniele.borio}@ec.europa.eu

***Abstract*—Digital signal processing for Global Navigation Satellite System (GNSS) receivers is mostly based on the assumption that the noise at the receiver input is Gaussian. This assumption leads to a non-linear Least Squares (LS) problem where GNSS signal parameters are estimated by minimizing a quadratic cost function. The receiver performance can be however significantly degraded by non-Gaussian phenomena such as interference and jamming.**

This paper reviews robust signal processing concepts and describes two approaches for the design of robust techniques for GNSS signal reception. Specific focus is devoted to M-estimators where the standard quadratic cost function considered by acquisition and tracking is replaced by the sum of less rapidly increasing functions. Using the M-estimator approach, robust versions of the standard acquisition and tracking blocks are obtained. The second approach is based on non-linear filters such as the median and the myriad filters. These filters are used to design robust correlation blocks.

A case study involving real data is used to demonstrate the effectiveness of robust signal processing techniques which have the potential to significantly improve the performance of GNSS receivers in the presence of non-Gaussian phenomena such as interference.

I. Introduction

GNSS receivers are usually designed on the assumption that the input samples provided by the receiver front-end and the final GNSS measurements are corrupted by Gaussian noise [1], [2]. Acquisition and tracking, the main signal processing blocks of a GNSS receiver, are, for example, designed under the hypothesis that the noise affecting the input samples is Gaussian. This assumption leads to a non-linear LS problem where GNSS signal parameters are estimated by minimizing a quadratic cost function.

In a similar way, the user Position, Velocity and Time (PVT) solution is computed solving a Weighted Least Squares (WLS) problem which can be directly derived from the hypothesis that pseudoranges and Doppler measurements are affected by errors characterized by a Gaussian probability density function (pdf) [1].

Received GNSS signals are however weak and signal reception can be affected by several impairments such as multipath and interference. In the presence of interference, an unwanted and, in general, non-Gaussian signal component is present at the receiver antenna: this component can significantly reduce the performance of a GNSS receiver. Jamming, in particular, is a special type of interference where powerful signals are broadcast in the GNSS frequency bands with the ultimate goal of preventing GNSS signal reception [3]. In the presence of interference, the hypothesis of input Gaussian noise may not be valid and the receiver performance may be significantly degraded.

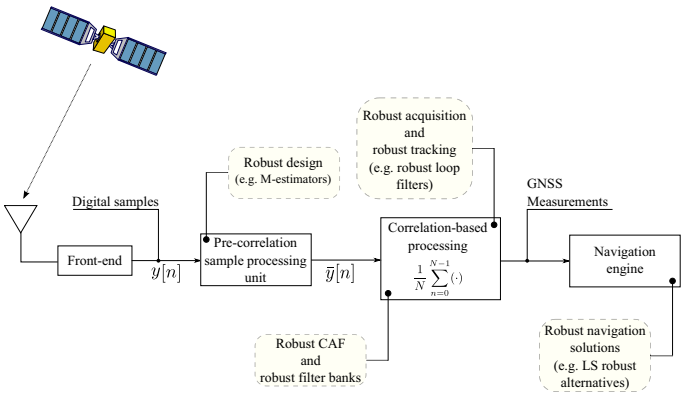

Fig. 1. Design of a robust GNSS receiver: functional blocks where robust techniques can be applied.

Unwanted non-Gaussian effects and interference can be effectively mitigated by the usage of robust statistical approaches and robust signal processing schemes [4], [5] which received significant interest over the last four decades. In this context, a technique is considered robust if it is able to effectively deal with model uncertainties and model mismatches. In particular, the performance of a robust technique is only marginally degraded when operating in conditions deviating from the design assumptions [5].

Several approaches exist to design robust processing schemes where the assumption of Gaussian input noise is relaxed and the LS principle is replaced by less sensitive criteria, such as the minmax approach [4] where the worst case scenario is considered.

Robust approaches can be employed at different stages of the receiver as shown in Fig. 1. Robust approaches can be used to design pre-correlation sample processing techniques which can reduce the impact of pulsed interference and outliers. This approach is investigated in Section III. Moreover, the classical correlator, which is based on 'mean' operator, can be replaced by robust alternatives such as the median [6], [7] and the myriad [8]. Robust design techniques can be used to design robust versions of the standard acquisition and tracking blocks. Finally, robust estimation approaches, no longer based on the LS technique, can be adopted to obtained 'robust' navigation solutions which are only marginally affected by outliers in the GNSS measurements [9].

978-1-5090-5922-5/17/$31.00 ©2017 European Union

Although robust signal processing techniques have the potential to significantly improve the performance of GNSS receivers in the presence of non-Gaussian phenomena such as interference, their usage has been quite limited. In particular, robust approaches have been recently considered for the computation of the user position where robust techniques have been used for the processing of GNSS observables [9]. These approaches provide significant performance improvements in the presence of multipath errors and outliers in the pseudorange measurements [9].

The paper investigates the usage of robust signal processing techniques at the sample level with specific focus on their application to GNSS signal acquisition and tracking. Two general approaches are discussed for the design of robust acquisition and tracking schemes: the first is based on the M-estimator framework [10], [11] and leads to the design of pre-correlation techniques able to significantly reduce the impact of pulsed interference. The second approach introduces robustness by directly acting on the filter bank (correlator) structure of acquisition and tracking. In particular, standard filters/correlators are replaced by robust alternatives such as the median and the myriad filters. Special attention is given to robust filter banks operating on complex input samples [6], [7].

The M-estimator and robust filter bank approaches are practically analysed using the data collected in [12] where GNSS samples are affected by jamming. Since the front-end used for the data collection is narrowband, the jamming signal periodically enters and exits the receiver input band. Thus, it is perceived as pulsed interference and the input samples result contaminated by outliers.

From the analysis it emerges that robust approaches enable receiver operations event in the close proximity of a jammer. In this respect, the approaches considered are effective tools for the design of advanced and computationally efficient techniques enabling GNSS signal reception even in the presence of significant levels of interference.

The remainder of this paper is organized as follows: Section II briefly reviews standard signal processing principles for GNSS. The M-estimator approach is considered in Section III whereas the robust filter bank framework is introduced in Section IV. The experimental setup is described in Section V and experimental results are presented in Section VI. Conclusions are finally drawn in Section VII.

II. Signal Processing for GNSS

The signal collected by the antenna of a GNSS receiver can be modelled as [1]:

$$y(t) = \sqrt{2C} d\left(t-\tau_0\right) c\left(t-\tau_0\right) \cos\left(2\pi(f_{RF}+f_0)t+\varphi_0\right) + \eta(t) \tag{1}$$

where

- C is the received signal power;
- $d(\cdot)$ is the navigation message;
- $c(\cdot)$ is a pseudo-random sequence extracted from a family of quasi-orthogonal codes modulated using rectangular pulses. $c(\cdot)$ accounts here also for the effect of the signal subcarrier [13];
- τ_0, f_0 and φ_0 are the delay, Doppler frequency and phase introduced by the communication channel;
- f_{RF} is the signal centre frequency;
- $\eta(t)$ is a zero-mean noise process.

Although several GNSS signals are simultaneously recovered by the GNSS receiver, a single component is considered in (1). Each GNSS signal is characterized by a specific pseudo-random sequence extracted from a family of quasi-orthogonal codes. In this way, the receiver is able to process each signal independently. This justifies the model assumption adopted in (1).

After filtering, down-conversion and digitization, signal (1) becomes a digital sequence:

$$y[n] = \sqrt{C}\tilde{d}\left(nT_s-\tau_0\right)\tilde{c}\left(nT_s-\tau_0\right)\mathrm{e}^{j2\pi f_0 nT_s+j\varphi_0}+\eta_{BB}[n] \tag{2}$$

where the notation '$x[n]$' is used to denote a discrete-time sequence sampled at the frequency $f_s = \frac{1}{T_s}$. The subscript "BB" denotes a base-band signal and symbol $\tilde{\cdot}$ is used to indicate that the useful signal component may be filtered by the receiver front-end.

$\eta_{BB}[n]$ is a noise term which is obtained from the processing of $\eta(t)$ in (1) and accounts for possible front-end disturbances such as quantization noise. A common hypothesis is to assume $\eta_{BB}[n]$ as an Additive White Gaussian Noise (AWGN) with real and imaginary parts each with variance, σ^2. This assumption may not be validy in the presence of interference or other impairments.

Under the Gaussian assumption, variance σ^2 is usually modelled as

$$\sigma^2 = N_0 B_{Rx} \tag{3}$$

where B_{Rx} is the front-end one-sided bandwidth and N_0 is the Power Spectral Density (PSD) of the input noise, $\eta(t)$. The ratio between the carrier power, C, and the noise power spectral density, N_0, defines the Carrier-to-Noise Power Spectral Density Ratio (C/N_0), one of the main signal quality indicators used in GNSS.

A. Standard Receiver Processing

The main goals of the signal processing blocks of a GNSS receiver are to detect the signal presence and estimate the signal parameters, τ_0, f_0 and φ_0. Under the assumption of Gaussian input noise, the estimation process is based on the minimization of the non-linear LS cost function

$$J\left(\tau, f_d, \varphi\right) = \sum_{n=0}^{N-1} \left| y[n] - Ac\left(nT_s-\tau\right)\mathrm{e}^{j2\pi f_d nT_s+j\varphi}\right|^2 \tag{4}$$

where N is the number of samples used during the estimation process and A accounts for the unknown signal amplitude. The product, $T_c = NT_s$ defines the coherent integration time. Cost function (4) is obtained applying the Maximum Likelihood

Estimator (MLE) approach [14] to the samples in (2) and adopting the Gaussian model for the noise samples, $\eta_{BB}[n]$. In this way, the signal parameters are estimated as:

$$\left\{\hat{\tau}, \hat{f}_d, \hat{\varphi}\right\} = \arg \min_{\tau, f_d, \varphi} J\left(\tau, f_d, \varphi\right) \tag{5}$$

where $\hat{\tau}$, $\hat{f}_d$, $\hat{\varphi}$ denote the final signal estimates.
Standard acquisition and tracking algorithms implement minimization (5): acquisition determines the signal presence and provides raw estimates of the code delay and Doppler frequency; signal tracking refines the minimization process using a gradient descent/ascent approach. Tracking also determines the carrier phase and tracks variations in the signal parameters. By expanding (4) and removing terms constant with respect to the signal parameters, it possible to show that minimization (5) is equivalent to the following maximization problem:

$$\left\{\hat{\tau}, \hat{f}_d, \hat{\varphi}\right\} = \arg \max_{\tau, f_d, \varphi} \sum_{n=0}^{N-1} \Re\left\{y[n] c\left(nT_s - \tau\right) \mathrm{e}^{-j2\pi f_d n T_s - j\varphi}\right\}. \tag{6}$$

In this case, the function maximized does not depend on A. Moreover the maximization with respect to φ can be performed explicitly. In particular,

$$\begin{aligned} &\max_{\varphi} \sum_{n=0}^{N-1} \Re\left\{y[n] c\left(nT_s - \tau\right) \mathrm{e}^{-j2\pi f_d n T_s - j\varphi}\right\} \\ &= \max_{\varphi} \Re\left\{\left[\sum_{n=0}^{N-1} y[n] c\left(nT_s - \tau\right) \mathrm{e}^{-j2\pi f_d n T_s}\right] \mathrm{e}^{-j\varphi}\right\} \\ &= \left|\sum_{n=0}^{N-1} y[n] c\left(nT_s - \tau\right) \mathrm{e}^{-j2\pi f_d n T_s}\right| = \left|C(\tau, f_d)\right| \end{aligned} \tag{7}$$

where

$$C(\tau, f_d) = \sum_{n=0}^{N-1} y[n] c\left(nT_s - \tau\right) \mathrm{e}^{-j2\pi f_d n T_s} \tag{8}$$

is the Cross-Ambiguity Function (CAF) [1]. Standard acquisition and tracking algorithms are designed to maximize the CAF which is computed using a bank of correlators.

III. M-Estimators and Robust CAF

Under the Gaussian hypothesis, the non-linear LS problem defined by cost function (4) is obtained. This type of problem is not robust in the sense that even a single outlier present in the input samples, $y[n]$, can significantly bias the cost function, seriously compromising the estimation process. A possible solution is to replace the squares in (4) with less rapidly increasing functions of the residuals [11], [15]:

$$r[n] = y[n] - Ac\left(nT_s - \tau\right) \mathrm{e}^{j2\pi f_d n T_s + j\varphi}. \tag{9}$$

In this way, robust versions of cost function (4) are obtained:

$$J_\rho\left(\tau, f_d, \varphi\right) = \sum_{n=0}^{N-1} \rho\Big(y[n] - Ac\left(nT_s - \tau\right) \mathrm{e}^{j2\pi f_d n T_s + j\varphi}\Big) \tag{10}$$

where $\rho(\cdot)$ is a positive function of complex argument

$$\rho(\cdot) : \mathbb{C} \to \mathbb{R}^+. \tag{11}$$

$\rho(\cdot)$ is usually symmetric with respect to its argument and is zero only of its argument is zero. A possible approach for the selection of $\rho(\cdot)$ is the M-estimator framework suggested by Huber [10], [11]. In particular, $\rho(\cdot)$ can be selected as

$$\rho(z) = -\log f(z) \tag{12}$$

where $f(z)$ is the pdf of possibly heavily-tailed complex random variables. When

$$f(z) = \frac{1}{2\pi\sigma^2} \exp\left\{-\frac{1}{2\sigma^2}|z|^2\right\}$$

is selected, the standard LS problem discussed in Section II is obtained. Heavily-tailed distributions may be more adequate to deal with outliers originating for example from the presence of interference. Example of such distributions are the Laplace and the Cauchy [6], [16] pdfs. Differently from the LS case, cost function (10) cannot be directly expanded and, in order to obtain a problem similar to (6), a different approach has to be adopted. In particular, it is necessary to exploit the fact that received GNSS signals are weak and the signal amplitude, A, assumes reduced values. Under this hypothesis, it is possible to expand $\rho(\cdot)$ in Taylor series with respect to A and approximate $J_\rho\left(\tau, f_d, \varphi\right)$ as [16]:

$$\begin{aligned} &J_\rho\left(\tau, f_d, \varphi\right) \approx \\ &\sum_{n=0}^{N-1} \Big[\rho\Big(y[n]\Big) - A\Re\left\{\rho_z(y[n]) c\left(nT_s - \tau\right) \mathrm{e}^{-j2\pi f_d n T_s - j\varphi}\right\}\Big]. \end{aligned} \tag{13}$$

In (13), $\rho_z(y[n])$ is the complex derivative of $\rho(\cdot)$ and it is defined as

$$\rho_z(y[n]) = \rho_I(y[n]) + j\rho_Q(y[n]) = \frac{\partial}{\partial y_I}\rho(y[n]) + j\frac{\partial}{\partial y_Q}\rho(y[n]) \tag{14}$$

where y_I and y_Q are used to denote the real and imaginary parts of the argument of $\rho(\cdot)$.
Using (13), it is finally possible to define robust estimates of the signal parameters through the maximisation of

$$\left\{\hat{\tau}, \hat{f}_d, \hat{\varphi}\right\} = \arg \max_{\tau, f_d, \varphi} \sum_{n=0}^{N-1} \Re\left\{\rho_z(y[n]) c\left(nT_s - \tau\right) \mathrm{e}^{-j2\pi f_d n T_s - j\varphi}\right\}. \tag{15}$$

Problem (15) is analog to (6) where the samples are at first pre-processed using the complex non-linearity $\rho_z(\cdot)$.
Similarly, to the LS case, the approach detailed above naturally leads to the concept of robust CAF which can be obtained

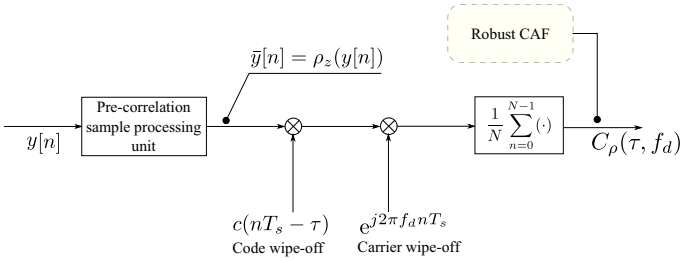

Fig. 2. Robust CAF obtained using a pre-correlation sample processing block. The pre-processing function, $\rho_z(\cdot)$, is obtained using the M-estimator framework.

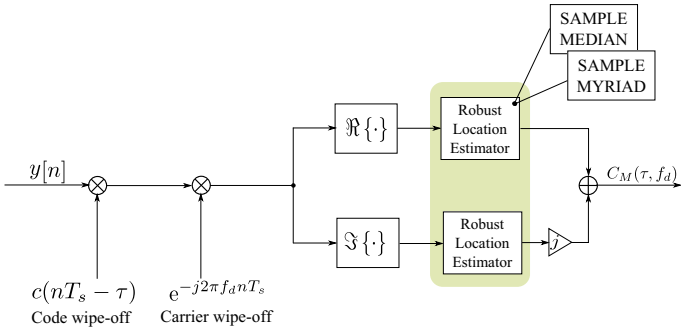

Fig. 3. Robust CAF obtained using the filter bank approach. Correlation is implemented using robust operators such as the sample median or the sample myriad.

through the explicit maximization with respect to φ. In particular,

$$\begin{aligned}\left\{\hat{\tau}, \hat{f}_d\right\} &= \arg\max_{\tau, f_d} \left| \sum_{n=0}^{N-1} \rho_z(y[n]) c\left(nT_s - \tau\right) \mathrm{e}^{-j2\pi f_d nT_s} \right| \\ &= \arg\max_{\tau, f_d} |C_\rho(\tau, f_d)| \\ \hat{\varphi} &= \angle C_\rho(\hat{\tau}, \hat{f}_d)\end{aligned} \tag{16}$$

with

$$C_\rho(\tau, f_d) = \sum_{n=0}^{N-1} \rho_z(y[n]) c\left(nT_s - \tau\right) \mathrm{e}^{-j2\pi f_d nT_s} \tag{17}$$

being a robust version of the CAF.
The robust CAF can be obtained using the processing scheme depicted in Fig. 2 where the input samples, $y[n]$, are at first pre-processed using the $\rho_z(\cdot)$ non-linearity. The M-estimator approach provides an effective framework for the design of pre-correlation interference mitigation techniques.

A. Complex Sign Non-linearity

Robustness can be obtained by considering the pdf of a complex Laplace distribution [16]. In this way, the following non-linearity is obtained [16]:

$$\bar{y}[n] = \rho_z(y[n]) = \frac{y[n]}{|y[n]|}. \tag{18}$$

This operation consists in normalizing each input sample by its amplitude. In this way, only the complex sign, i.e. the complex exponential of signal phase, is retained. When a strong outlier is present in the input samples, normalization (18) strongly reduces its impact.
An analysis of the complex sign non-linearity can be found in [16].

B. The Myriad Non-linearity

A second type of non-linearity can be obtained by considering a complex Cauchy distribution. In this case, the following non-linearity is obtained [17]:

$$\bar{y}[n] = \rho_z(y[n]) = \frac{Ky[n]}{K + |y[n]|^2} \tag{19}$$

where K is selectable and it is usually called linearity parameter [6]. Function (19) has been denoted 'myriad non-linearity' for its connection with the sample myriad [8]. The sample myriad is obtained as robust location estimator in the presence of Cauchy noise. K is denoted as linearity parameter since it controls the level of non-linearity introduced by (19). For $K \to \infty$, $\rho_z(\cdot)$ converges to the identity and no robustness is introduced in the system. In this respect, the performance of the myriad non-linearity strongly depends on K: if K is too large, no robustness is introduced. On the contrary, small values of K may lead to significant distortions to the input samples.
The selection of K is still an open problem and it usually depends on the probability of occurrence and on the power of the outliers present in the input samples. In [17], it is shown that K should be proportional to the variance of $y[n]$ estimated in the absence of outliers. Moreover, it was shown that $K = 6\sigma^2$ (with σ^2 defined in (3)) produces good results for the scenario considered. For this reason, $K = 6\sigma^2$ is adopted in the remainder of this paper.

IV. Robust Filter Banks

A second approach to obtain robust versions of the CAF is to note that each correlator output can be interpreted as an estimator for the signal amplitude after code and carrier wipe-off. In this respect, standard correlation processing can be interpreted as a location estimator [11], [6]. CAF in (8) is the results of the summation of the samples after code and carrier removal. This summation can be interpreted as a mean scaled by N, the number of samples used for the CAF computation. Note that scaling does not change the results of the processing implemented in acquisition and tracking. In this respect, different definition of the CAF exist with different scaling factors.
Using this principle, robust correlators are obtained by replacing the summation (sample mean) required for the computation of the CAF with robust location parameter estimators such as the sample median and the sample myriad [6]. This principle is illustrated in Fig. 3 which shows a robust correlator implemented using either the sample median or the sample myriad. Note that acquisition and tracking require the computation

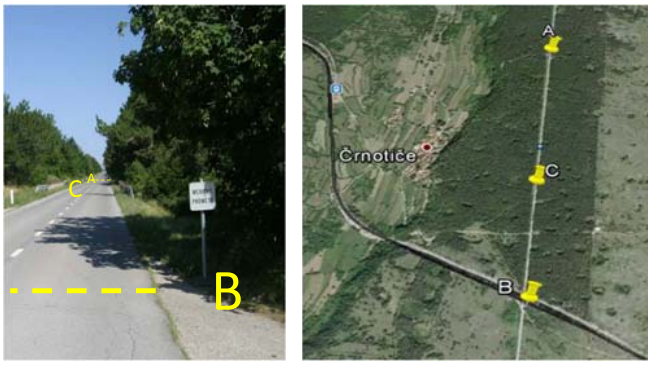

Fig. 4. Environment selected for the tests in the presence of jamming. In order to minimize the impact of the jammer on other GPS users, a remote area close to Črnotiče, Slovenia, was selected as location for the data collection.

of several correlators in parallel. Each correlator can be interpreted as a filter. Thus, when robust operators are used, a robust filter bank is obtained. For this reason, this technique is denoted here as robust filter bank approach.
It is noted that in Fig. 3, the real and imaginary parts of the samples after code and carrier wipe-off are treated separately. In this way, the phase-coupled complex median/myriad approach [6], [7] is implemented.
Thus, the robust filter bank CAF is obtained as

$$C_M(\tau, f_d) = \mathrm{ROP}_{n=0}^{N-1}\left[\Re\left\{y[n]c\left(nT_s-\tau\right)\mathrm{e}^{-j2\pi f_d nT_s}\right\}\right] + j\mathrm{ROP}_{n=0}^{N-1}\left[\Im\left\{y[n]c\left(nT_s-\tau\right)\mathrm{e}^{-j2\pi f_d nT_s}\right\}\right] \quad (20)$$

where $\mathrm{ROP}_{n=0}^{N-1}$ is a robust operator, for example, the median or the myriad, using the samples from 0 to $N-1$.
In the following, both median and myriad operators have been considered. The myriad computation has been implemented using "Algorithm II" detailed in [18].

V. Experimental Setup

In order to experimentally evaluate the benefits brought by the robust signal processing techniques introduced in the previous sections, the data collected during the experiments described in [19], [12] were used. This type of experiments had the primary goal of assessing the impact of jamming in a realistic road environment and to test different detection approaches [19]. Data collections were performed in Črnotiče, Slovenia in collaboration with the University of Ljubljana, Faculty of Maritime Studies and Transport, Portoroz, Slovenia. The tests were conducted in July 2015 along a straight road. A view of the environment considered for the tests is shown in Fig. 4. During the test considered here, a battery-powered jammer [20] emitting a power of about 9 dBm was mounted on a car which was periodically passing in front of a measurement unit placed on the side of the road. Additional details on the jammer used for the experiment can be found in [19]. The measurements unit consisted of a Software Defined Radio (SDR) front-end and of a commercial GPS receiver, a u-blox LEA-6T receiver mounted according

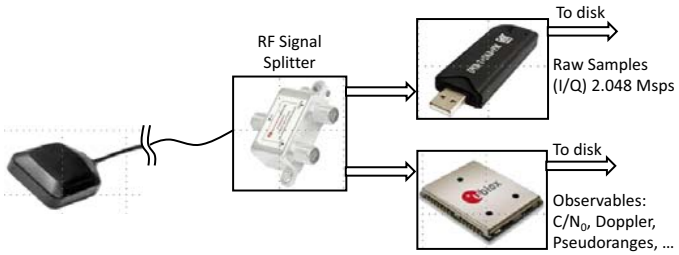

Fig. 5. Measurement unit adopted for the data collection: a RTL2832u tv tuner was used to collect raw IQ data whereas a u-blox LEA-6T receiver provided GPS observables.

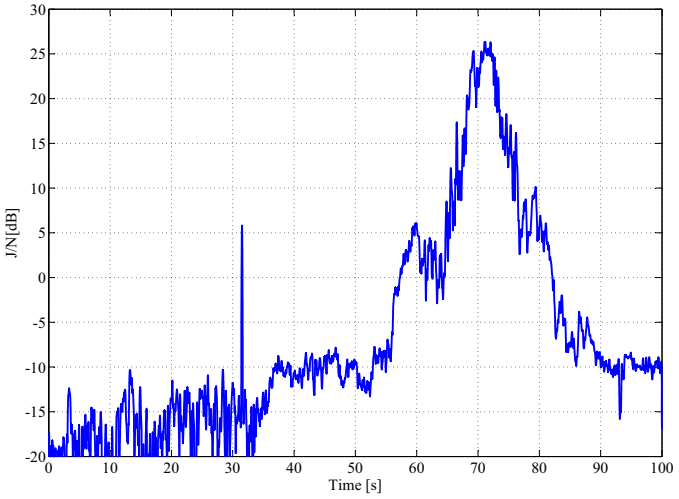

Fig. 6. J/N estimated during the car test. A maximum J/N of about 25 dB is observed when the jammer is in the close proximity (about 5 metres) of the measurement unit.

to the configuration depicted in Fig. 5. The front-end was a low-cost, narrow band TV tuner, the Realtek RTL2832u with a maximum sampling frequency equal to 2.048 MHz. This sampling frequency is sufficient to capture the main lobe of GPS signals and it is significantly lower than the frequency band, $(1563.8\text{MHz} - 1580.6\text{MHz})$, spanned by the jamming signal. In this way, the jamming signal periodically enters and exits the receiver band and it is thus perceived as a form of pulsed interference.
The experiment with the moving car was designed to simulate different Jammer-to-Noise Power Ratio (J/N) conditions. In particular, when the car is far from the measurement unit, the jamming signal is so attenuated that the reception of GPS signals is not affected. The received jamming power progressively increases as the car approaches the measurement unit. During the experiment, a minimum distance of about 5 was obtained between the jammer and measurement unit. In order to provide an indication of the strength of the received jamming signal, the J/N was estimated using the collected samples. The collected data were divided in blocks of 1 ms. The total received power was estimated as the sample variance of each data block. The noise variance was determined using the samples at the beginning of the dataset. These samples

TABLE I
PARAMETERS OF THE SAMPLES PROVIDED BY THE RTL2832U FRONT-END AND SETTINGS ADOPTED FOR THE TRACKING LOOPS.

Parameter	Value
Sampling frequency, f_s	2.048 MHz
Sampling type	Complex IQ
Number of bits	8
Coherent integration time	1 ms
DLL order	2nd
PLL order	3rd
DLL bandwidth	5 Hz
PLL bandwidth	25 Hz
Eearly-Late spacing	1 chip

were collected when the jammer was far from the victim receiver. The jamming power was estimated as the difference between the total power and the noise variance. When the jammer is in the close proximity of the jammer, a J/N of about 25 dB is observed. This is a significant level of interference.

The custom Matlab software receiver described in [12] was used for processing the data collected. The different robust approaches detailed in Sections III and IV were implemented and tested using the datsets collected in Črnotiče.

The parameters of the samples provided by the RTL2832u front-end and the settings adopted for the tracking loops used for the processing are briefly summarized in Table I. The RTL2832u front-end is characterized by a poor quality local oscillator which introduces a significant clock drift. For this reason large bandwidths are required for the Phase Lock Loop (PLL) and Delay Lock Loop (DLL) design.

VI. REAL DATA ANALYSIS

Experimental results obtained processing the data described in Section V are discussed in this section. In particular, tracking results are at first briefly analysed for each processing scheme. A comparison in terms of effective C/N_0 [21] is then provided in Section VI-F.

A. Standard Processing

Tracking results obtained using standard processing are shown in Fig. 7. At the beginning of the test, the car is far from the jammer and the receiver is able to properly track the GPS signal. The Early and Late correlators used in tracking are properly aligned and the Prompt correlator has a magnitude greater than that of the other two. This fact is clearly shown in Fig. 7 a). After 60 seconds, the car starts approaching the jammer and the receiver performance starts degrading. In particular, standard processing is unable to maintain phase and delay lock. Loss of phase lock is observed in Fig. 7 b) which shows the In-phase/Quadrature (IQ) components of the Prompt correlator. Under phase lock conditions, most of the signal energy is concentrated in the in-phase component (blue line in Fig. 7 b)): in the proximity of the jammer the signal energy is equally split between the in-phase and quadrature components. Loss of loss can be also observed in Fig. 7 c) which provides the Doppler frequency and the code delay estimated by the

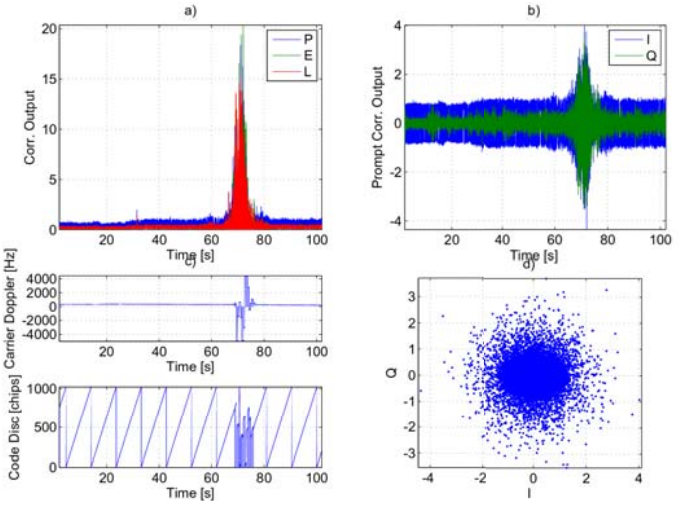

Fig. 7. Results obtained using standard processing. 1) Amplitude of the Prompt, Early and Late correlators. b) IQ components of the Prompt correlator. c) Estimated carrier Doppler shift and code delay (modulo the code length). d) Scatter plot of the Prompt correlator.

receiver. In the proximity of the jammer, the receiver is unable to correctly estimate the signal parameters. For this reason, significant discontinuities are observed in Fig. 7 c). Finally, Fig. 7 d) provides the scatter plot described by the Prompt correlator: due to jamming it is not possible to distinguish the two clouds defined by the Binary Phase Shift Keying (BPSK) modulation adopted by the GPS Coarse Acquisition (C/A) signal.

These results show that standard processing is unable to operate in the presence of jamming.

B. Complex Sign Non-Linearity

The same dataset considered in Section VI-A has been processed using the complex sign non-linearity described in Section VI-B. Sample tracking results are provided in Fig. 8. In this case, the receiver is able to maintain signal lock during the whole duration of the experiment and even in the close proximity of the jammer. This fact clearly emerges from Fig. 8. From Fig. 8 a), in particular, it is possible to note that the amplitude of the three correlators progressively decreases as the jamming power becomes stronger. This is due to the fact that, in practice, the complex sign non-linearity only retains the phase information. When the jamming power is strong, the correlation between the phase of the input samples and that of the locally generated signals becomes weak resulting in reduced correlator amplitudes. Despite this fact, the complex sign non-linearity enable receiver processing and the power of the Prompt correlator remains concentrated in the in-phase branch as shown in Fig. 8 b). This fact clearly emerges also from Fig. 8 d) which provides the scatter plot of the Prompt correlator. Differently from the standard processing case, it is now possible to distinguish the two symbol clouds defined by the BPSK modulation. Finally, Fig. 8 c) provides the estimated Doppler shift and code delay: no discontinuity is observed

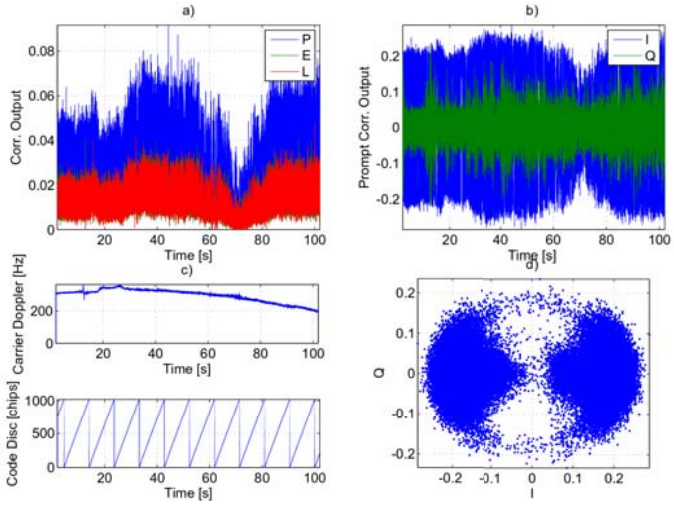

Fig. 8. Results obtained using the complex sign non-linearity. 1) Amplitude of the Prompt, Early and Late correlators. b) IQ components of the Prompt correlator. c) Estimated carrier Doppler shift and code delay (modulo the code length). d) Scatter plot of the Prompt correlator.

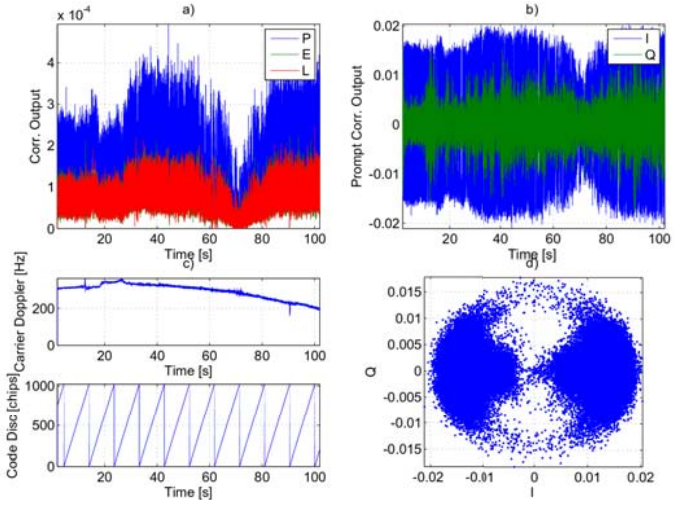

Fig. 9. Results obtained using the myriad non-linearity. 1) Amplitude of the Prompt, Early and Late correlators. b) IQ components of the Prompt correlator. c) Estimated carrier Doppler shift and code delay (modulo the code length). d) Scatter plot of the Prompt correlator.

during the whole dataset. This indicates the ability of the receiver to maintain lock on the signal parameters.

C. Myriad Non-Linearity

The experimental findings obtained using the Myriad non-linearity are provided in Fig. 9. For the processing, $K = 6\sigma^2$ was used where σ^2 was estimated from the samples at the beginning of the dataset when jamming was absent. The results obtained are similar to those observed in Section VI-B for the complex sign non-linearity. Pre-processing the samples significantly improves the robustness of the receiver which is able to operate even in the close proximity of the jammer.

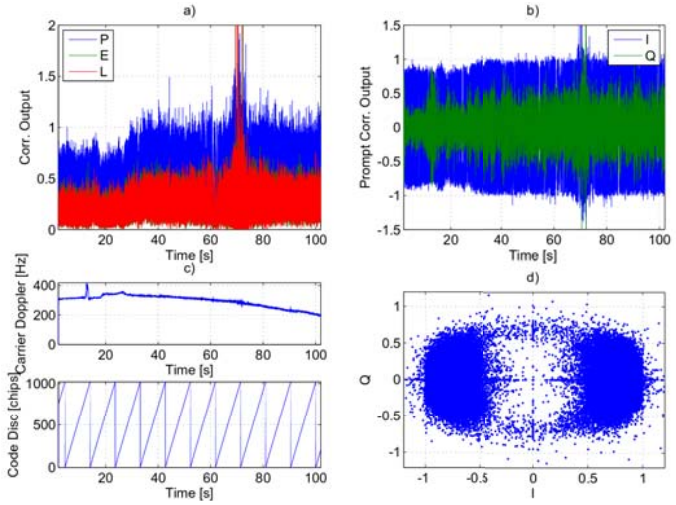

Fig. 10. Results obtained using the median correlator. 1) Amplitude of the Prompt, Early and Late correlators. b) IQ components of the Prompt correlator. c) Estimated carrier Doppler and code delay (modulo the code length). d) Scatter plot of the Prompt correlator.

D. Median Correlator

The median correlator is considered in Fig. 10. Although also this type of processing enable operations even in the close proximity of the jammer, it is possible to observe some differences with respect to the previous approaches. In particular, the amplitude of the correlator increases in the presence of strong jamming signals. This is due to the fact that the median operator is a selector. This implies that the output of the median is one of the input samples. When significant levels of interference are present, then also the sample selected by the median operator is, at least partially, corrupted by jamming. The spikes observable in Figs. 10 a) and b) may be the indication that the level of contamination caused by the jammer is close to the *breakdown point* of the median estimator. The breakdown point is the proportion of contaminated samples that an estimator can handle before producing incorrect estimates [11]. Since the car is moving, the victim receiver is exposed to significant levels of jamming only for a reduced period of time. In this experiment, the exposition time to critical levels of jamming is sufficiently short not to make the receiver loose lock. For this reason, no discontinuities are observed in the estimated Doppler shits and code delays provided in Fig. 10 c). Finally, as for the cases discussed in Sections VI-B and VI-C, the scatter plot of the Prompt correlator is shown in bottom right part of Fig. 10. Also in this case, it is possible to distinguish the clouds defined by the symbols of the BPSK modulation. It is also possible to observe a pattern, a sort of cross, where either the in-phase or quadrature component of the Prompt correlator is equal to zero. This pattern is also due to the fact that the median is a selector and that the input samples are quantized. Thus, there is a non-negligible probability that also the output samples are zero. This fact is reflected by the pattern in Fig. 10 d).

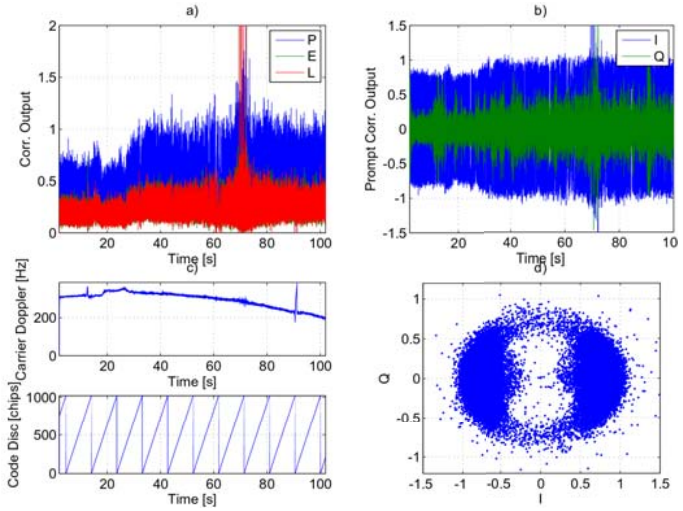

Fig. 11. Results obtained using the sample myriad correlator. 1) Amplitude of the Prompt, Early and Late correlators. b) IQ components of the Prompt correlator. c) Estimated carrier Doppler shift and code delay (modulo the code length). d) Scatter plot of the Prompt correlator.

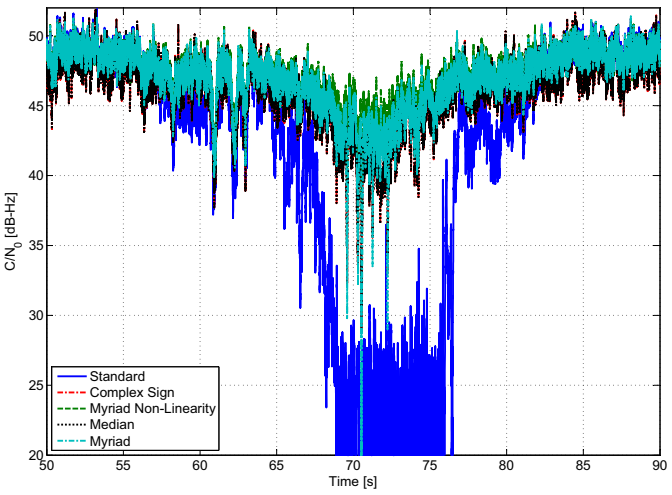

Fig. 12. Comparison between C/N_0 estimates obtained using different processing strategies.

E. Myriad Correlator

The myriad correlator is finally analysed in Fig. 11. As for the myriad non-linearity, $K = 6\sigma^2$ was selected. The sample myriad is not a selector and the patterns observed for the median correlator are no longer present. Despite this fact, the myriad correlator behaves similarly to the median. Also in this case, an increase of power is observed for the three correlators when the jamming power is maximum. Also in this case, however, the receiver is able to maintain signal lock during the whole duration of the experiment. Consistent Doppler frequency and code delay estimates are produced and it is possible to distinguish the symbol clouds defined by the BPSK modulation of the GPS C/A signal.

F. Comparison

In the previous sections, the different processing strategies were analysed singularly with respect to their ability to maintain signal lock and to produce consistent Doppler and delay estimates even in the close proximity of the jammer. In this section, the five strategies are compared in terms of effective C/N_0 [21]. As mentioned in Section II, the C/N_0 is one of the main signal quality indicator adopted in GNSS. The effective C/N_0 is the C/N_0 estimated by the receiver from the correlator outputs. Thus, the value it assumes effectively reflects the ability of the receiver to withstand and reject jamming and interference. The C/N_0 estimates obtained using the five processing strategies analysed above are compared in Fig. 12. As discussed in Section VI-A, standard processing is unable to maintain lock and to re-acquire the GPS signal in the $[67\text{s} - 77\text{s}]$ time interval. In this time range, low and inconsistent C/N_0 estimates are produced.
The four robust approaches considered are all able to maintain lock and outperform standard processing in the presence of strong levels of jamming. The best performance is obtained by the myriad non-linearity followed by the myriad correlator. The complex sign non-linearity and the median correlator lead to the same C/N_0 estimates which are however close (fractions of dBs) to the effective C/N_0 obtained for the other two robust approaches. It is noted that the median and the myriad correlators are significantly more computationally demanding than the use of non-linearities for the pre-processing of the input samples. The iterative procedure adopted for the computation of the sample myriad [18] is particularly computationally intensive. With this in mind and taking into account the results provided in Fig. 12, the use of non-linearities should be preferred to introduce robustness in GNSS signal processing.

VII. Conclusions

In this paper, two strategies for introducing robustness to GNSS signal processing were discussed. The first approach is derived from the M-estimator framework and consists in the introduction of a pre-processing unit which uses a non-linearity to reduce the impact of outliers in the input samples. The M-estimator framework was also adopted for the design of the non-linearities. Specifically, the complex sign and myriad non-linearities were analysed. The second approach was based on the introduction of robust operators for the evaluation of the correlation between the input samples and locally generated signal replicas. Robust filter banks were used for the evaluation of the signal correlation. The median and myriad correlators were introduced and analysed. In this way, a total of four robust approaches was considered.
The four approaches were empirically tested using data collected in the presence of jamming. From the analysis, it emerges that robust signal processing can significantly enhance the receiver performance in the presence of jamming. When robust techniques are applied, the receiver is able to maintain signal lock under conditions where standard processing is unable to operate. All robust approaches provided satisfactory

results even in the close proximity of the jammer when a J/N of about 25 dB was observed. The M-estimator approach based on the usage of a pre-processing unit is significantly less computationally demanding than the filter bank strategy. In this respect and in light of the fact that the two approaches provide similar performance, the usage of non-linearities should be preferred for the introduction of robustness in GNSS receiver algorithms.

REFERENCES

[1] E. D. Kaplan and C. Hegarty, Eds., *Understanding GPS: Principles and Applications*, 2nd ed. Norwood, MA, USA: Artech House Publishers, Dec. 2005.

[2] A. Van Dierendonck, "Ch. 5, GPS receivers," in *Global Positioning System Theory and Applications*, B. W. Parkinson and J. J. Spilker Jr., Eds. American Institute of Aeronautics & Astronautics, 1996, vol. 1, pp. 329–407.

[3] D. Borio, F. Dovis, H. Kuusniemi, and L. L. Presti, "Impact and detection of GNSS jammers on consumer grade satellite navigation receivers," *Proc. IEEE*, vol. 104, no. 6, pp. 1233–1245, Jun. 2016.

[4] S. A. Kassam and H. V. Poor, "Robust techniques for signal processing: A survey," *Proc. IEEE*, vol. 73, no. 3, pp. 433–481, Mar. 1985.

[5] A. M. Zoubir, V. Koivunen, Y. Chakhchoukh, and M. Muma, "Robust estimation in signal processing: A tutorial-style treatment of fundamental concepts," *IEEE Signal Process. Mag.*, vol. 29, no. 4, pp. 61–80, Jul. 2012.

[6] G. R. Arce, *Nonlinear Signal Processing: A Statistical Approach*. Wiley-Interscience, Nov. 2004.

[7] S. Hoyos, Y. Li, J. Bacca, and G. R. Arce, "Weighted median filters admitting complex-valued weights and their optimization," *IEEE Trans. Signal Process.*, vol. 52, no. 10, pp. 2776–2787, Oct. 2004.

[8] J. G. Gonzalez and G. R. Arce, "Optimality of the myriad filter in practical impulsive-noise environments," *IEEE Trans. Signal Process.*, vol. 49, no. 2, pp. 438–441, Feb. 2001.

[9] S. Zair, S. L. Hgarat-Mascle, and E. Seignez, "A-contrario modeling for robust localization using raw gnss data," *IEEE Trans. Intell. Transp. Syst.*, vol. 17, no. 5, pp. 1354–1367, May 2016.

[10] P. J. Huber, "Robust estimation of a location parameter," *Ann. Math. Statist.*, vol. 35, no. 1, pp. 73–101, Mar. 1964.

[11] P. J. Huber and E. M. Ronchetti, *Robust Statistics*, 2nd ed., ser. Wiley Probability and Statistics. John Wiley and Sons, Mar. 2009.

[12] D. Borio, "Swept GNSS jamming mitigation through pulse blanking," in *Proc. of the European Navigation Conference (ENC)*, May 2016, pp. 1–8.

[13] J. W. Betz, "Binary offset carrier modulations for radionavigation," *NAVIGATION, the Journal of the Institute of Navigation*, vol. 48, no. 4, pp. 227–246, Winter 2001.

[14] S. M. Kay, *Fundamentals of Statistical Signal Processing: Estimation Theory*. Pearson Education, 1993, vol. 1.

[15] X. Wang and H. V. Poor, "Robust multiuser detection in non-gaussian channels," *IEEE Trans. Signal Process.*, vol. 47, no. 2, pp. 289–305, Feb. 1999.

[16] D. Borio, "Robust GNSS signal processing: the complex sign non-linearity," *IEEE Trans. Aerosp. Electron. Syst.*, pp. 1–10, Nov. 2016, submitted for publication.

[17] ——, "Myriad non-linearity for GNSS robust signal processing," *IET Radar, Sonar & Navigation*, pp. 1–20, Jan. 2017, submitted for publication.

[18] S. Kalluri and G. R. Arce, "Fast algorithms for weighted myriad computation by fixed-point search," *IEEE Trans. Signal Process.*, vol. 48, no. 1, pp. 159–171, Jan. 2000.

[19] F. Dimc, D. Borio, C. Gioia, G. Baldini, M. Bažec, and M. Basso, "An experimental evaluation of low-cost GNSS jamming sensors," *NAVIGATION, the Journal of the Institute of Navigation, Accepted for publication*, pp. 1–14, Dec. 2016.

[20] R. H. Mitch, R. C. Dougherty, M. L. Psiaki, S. P. Powell, B. W. O'Hanlon, J. A. Bhatti, and T. E. Humphreys, "Signal characteristics of civil GPS jammers," in *Proc. of the 24th International Technical Meeting of The Satellite Division of the Institute of Navigation (ION GNSS)*, Portland, OR, Sep. 2011, pp. 1907–1919.

[21] J. W. Betz, "Effect of partial-band interference on receiver estimation of C/N_0: Theory," in *Proc. of the National Technical Meeting of The Institute of Navigation*, Long Beach, CA, Jan. 2001, pp. 817–828.